Version 3.0
October 2006

Wide Field Camera 3 Instrument Mini-Handbook for Cycle 16

For long-term planning only
Do not propose for WFC3 in Cycle 16

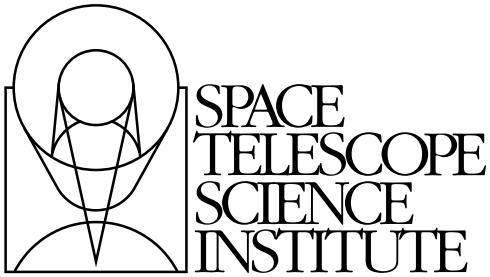

Space Telescope Science Institute
3700 San Martin Drive
Baltimore, Maryland 21218
help@stsci.edu

Operated by the Association of Universities for Research in Astronomy, Inc., for the National Aeronautics and Space Administration

User Support

For prompt answers to any question, please contact the STScI Help Desk.

- **E-mail:** help@stsci.edu
- **Phone:** (410) 338-1082
  (800) 544-8125 (U.S., toll free)

World Wide Web

Information and other resources are available on the WFC3 World Wide Web sites at STScI and GSFC:

- **URL:** http://www.stsci.edu/hst/wfc3
- **URL:** http://wfc3.gsfc.nasa.gov

WFC3 Mini-Handbook Revision History

Version	Date	Editor
3.0	October 2006	Howard E. Bond
2.0	October 2003	Massimo Stiavelli
1.0	October 2002	Mauro Giavalisco

Contributors:

Sylvia Baggett, Tom Brown, Howard Bushouse, Mauro Giavalisco, George Hartig, Bryan Hilbert, Randy Kimble, Matt Lallo, Olivia Lupie, John MacKenty, Larry Petro, Neill Reid, Massimo Robberto, Massimo Stiavelli.

Citation:

In publications, refer to this document as:
Bond, H. E., et al. 2006, "Wide Field Camera 3 Instrument Mini-Handbook, Version 3.0" (Baltimore: STScI)

Send comments or corrections to:
Space Telescope Science Institute
3700 San Martin Drive
Baltimore, Maryland 21218
E-mail:help@stsci.edu

Acknowledgments

The WFC3 Science Integrated Product Team (2006)

Sylvia Baggett
Howard Bond
Tom Brown
Howard Bushouse
George Hartig
Bryan Hilbert
Robert Hill (GSFC)
Jessica Kim Quijano
Randy Kimble (Instrument Scientist, GSFC)
John MacKenty (Deputy Instrument Scientist)
Larry Petro
Massimo Robberto
Megan Sosey

Past Science IPT Members

Wayne Baggett
Laura Cawley
Ed Cheng (GSFC, now Conceptual Analytics)
Ilana Dashevsky
Don Figer
Mauro Giavalisco
Shireen Gonzaga
Christopher Hanley
Ron Henry
Pat Knezek
Ray Kutina
Casey Lisse
Olivia Lupie
Peter McCullough
Neill Reid
Michael Robinson
Massimo Stiavelli

The WFC3 Scientific Oversight Committee

Bruce Balick, University of Washington
Howard E. Bond, Space Telescope Science Institute
Daniela Calzetti, Space Telescope Science Institute
C. Marcella Carollo, Institute of Astronomy, ETH, Zurich
Michael J. Disney, Cardiff University
Michael A. Dopita, Mt Stromlo and Siding Spring Observatories
Jay Frogel, AURA
Donald N. B. Hall, University of Hawaii
Jon A. Holtzman, New Mexico State University
Gerard Luppino, University of Hawaii
Patrick J. McCarthy, Carnegie Observatories
Robert W. O'Connell, University of Virginia (Chair)
Francesco Paresce, European Southern Observatory
Abhijit Saha, National Optical Astronomy Observatory
Joseph I. Silk, Oxford University
John T. Trauger, Jet Propulsion Laboratory
Alistair R. Walker, Cerro Tololo Interamerican Observatory
Bradley C. Whitmore, Space Telescope Science Institute
Rogier A. Windhorst, Arizona State University
Erick T. Young, University of Arizona

Thanks

The Editor thanks Susan Rose for her contributions to the production of this *Mini-Handbook*.

Table of Contents

List of Figures

List of Tables

Wide Field Camera 3

In this book. . .

1. Overview

1.1 General Information

The Wide Field Camera 3 (WFC3) is a fourth-generation instrument that is designed to be installed in the *Hubble Space Telescope* (*HST*) during Servicing Mission 4 (SM4). At this writing in early October 2006, the status of SM4 is uncertain in regard to whether it will occur, and if so when it will take place. Due to this uncertainty, the Space Telescope Science Institute (STScI) will not accept WFC3 observing proposals for Cycle 16 (which nominally covers *HST* observations to be conducted between July 2007 and June 2008). The purpose of this *Mini-Handbook*, therefore, is to provide basic information about the planned capabilities of WFC3, at a level that will be helpful to astronomers making long-range plans for future *HST* observing programs. A full-scale WFC3 *Instrument Handbook*, giving complete details of the instrument and its use, is planned to be issued at a later time to assist astronomers in preparing actual WFC3 observing proposals for a future Cycle. It should be noted that WFC3 is, at this writing, still under development. Although this *Mini-Handbook* is as accurate as possible, the information herein is still subject to possible changes.

The WFC3 instrument is designed to occupy *HST*'s radial scientific-instrument bay, where it will obtain on-axis direct images. During SM4, if it occurs, the shuttle astronauts will install WFC3 in place of the currently available Wide Field Planetary Camera 2 (WFPC2).

WFPC2, in turn, was installed during SM1 in December 1993, to replace the original Wide Field/Planetary Camera (WF/PC1). WFPC2, like WFC3, contains optics that correct for the spherical aberration discovered in the *HST* primary mirror following launch of the telescope in April 1990.

WFC3 uses some components of the original WF/PC1, which will thus see service once again onboard *Hubble* if there is a successful SM4. WFC3 is designed to ensure that *HST* maintains its unique imaging capabilities until the end of its mission, while at the same time advancing its survey and discovery capability due to its combination of wide wavelength coverage, wide field of view, and high sensitivity. WFC3 would also provide a good degree of redundancy for the aging Advanced Camera for Surveys (ACS) and Near-Infrared Camera and Multi-Object Spectrometer (NICMOS) cameras.

A key feature of WFC3 is its panchromatic wavelength coverage. By combining two optical/ultraviolet CCDs with a near-infrared HgCdTe array, WFC3 will be capable of direct, high-resolution imaging over the entire wavelength range from 200 to 1700 nm. Equipped with a comprehensive range of wide-, intermediate-, and narrow-band filters, WFC3 will have broad applicability to a variety of new astrophysical investigations.

WFC3 is a facility instrument. It is being developed, constructed, characterized, and calibrated by an Integrated Product Team (IPT) led by NASA's Goddard Space Flight Center (GSFC), and composed of staff astronomers and engineers from GSFC, STScI, Ball Aerospace & Technologies Corp., the Jet Propulsion Laboratory (JPL), and other industrial contractors.

A Scientific Oversight Committee (SOC), selected by NASA from the international astronomical community and appointed in 1998, provides scientific advice for the design and development of WFC3. The SOC's activities have been in a variety of areas, including: definition of the key scientific goals and success criteria for WFC3; participation in project reviews; recommending an optimum set of filters and grisms for the instrument and the pixel scale and field of view of the detectors; participation in the selection of flight detectors; and advice on technical trade-off decisions in the light of the scientific goals of the instrument. The SOC continues to provide oversight on all aspects of WFC3 development, with the aim of assuring that the camera will achieve its scientific goals.

1.2 Key Features of Wide Field Camera 3

The optical design of WFC3 features two independent channels, one sensitive at ultraviolet (UV) and optical wavelengths, approximately 200 to 1000 nm (the UVIS channel), and the other sensitive at near-infrared (near-IR) wavelengths, approximately 900 to 1700 nm (the IR channel). A channel-selection mirror will direct on-axis light from the *HST* Optical

Telescope Assembly (OTA) to the IR channel, or can be removed from the beam to allow light to enter the UVIS channel. This means that *simultaneous* observations with the UVIS and IR detectors are not possible. However, it is anticipated that both UVIS and IR observations can be made sequentially during the same *HST* orbit.

The extended wavelength range, combined with high sensitivity, high spatial resolution, large field of view, and a wide selection of spectral elements, make WFC3 an extremely versatile instrument. Key features of WFC3 include:

- UVIS channel: two 2k×4k CCDs; pixel scale 0.04 arcsec/pix; field of view 163×164 arcsec; wavelength range 200-1000 nm; S/N=10 in a 10-hour exposure (F606W filter) for a point source with V=28.9.
- IR channel: 1k×1k HgCdTe array; pixel scale 0.13 arcsec/pix; field of view 123×137 arcsec; wavelength range 900-1700 nm; S/N=10 in a 10-hour exposure (F160W) for a point source with H=28.0.
- 62 broad-, medium-, and narrow-band filters in the UVIS channel.
- 15 broad-, medium-, and narrow-band filters in the IR channel.
- 1 grism in the UVIS channel, and 2 grisms in the IR channel.

A "white paper," prepared by the SOC and the Science IPT, outlines the scientific areas that will benefit most from the capabilities of WFC3. These include searches for galaxies at redshifts up to z~10; studies of the physics of star formation in distant and nearby galaxies; investigations of resolved stellar populations down to faint levels in the UV, optical, and near-IR; and high-resolution imaging of objects in the solar system. Of particular interest will be programs that fully exploit the panchromatic capability of WFC3 for broad investigations of the assembly and evolution of galaxies; star birth, evolution, and death and its relation to the interstellar medium; and meteorology of the outer planets. The white paper (Stiavelli, M., & O'Connell, R.W., eds., 2000, "*Hubble Space Telescope* Wide Field Camera 3, Capabilities and Scientific Program") can be found at:

http://wfc3.gsfc.nasa.gov/white_paper.html

1.3 Current Instrument Status

At present (October 2006), as the editing of this *Mini-Handbook* was being completed, WFC3 continues to be developed and tested as we await a decision to proceed with SM4.

At the time of the January 2004 decision to cancel SM4, WFC3 was reaching the end of its assembly stage. To characterize the state of the instrument at that time, NASA directed the WFC3 program to conduct a "characterization" system-level thermal-vacuum test of the instrument. The instrument proceeded into this test in the fall of 2004. This was done in

spite of a significant number of known issues, which normally would have been resolved prior to a full acceptance/qualification thermal-vacuum test.

The fall 2004 testing successfully demonstrated the overall operation and performance of the instrument, and it informs the performance predictions in this *Mini-Handbook*. Subsequently, with improving prospects for an SM4, WFC3 has been partially disassembled to resolve both the previously known issues and additional items discovered during testing. In particular, the following problems have been addressed: significant ghost images were discovered in some of the UVIS filters and have been eliminated by replacing the affected filters; various electronics issues have been resolved; and the thermal control system has been improved. A flight UVIS detector has been selected, and a superior infrared detector (FPA 129) has been produced and is a strong candidate for flight.

At this writing, WFC3 is expected to resume thermal-vacuum testing early in 2007, if authority to proceed with SM4 is granted.

1.4 The WFC3 Instrument Team at STScI

STScI maintains a team of Instrument Scientists, Data Analysts, Engineers, and Scientific Programmers, who support the design, development, operation, calibration, and documentation of WFC3. STScI also maintains a Help Desk to provide answers quickly to any WFC3- and *HST*-related questions. Please send all questions regarding WFC3 and *HST* to the Help Desk, as follows:

- E-mail: help@stsci.edu
- Phone: (410) 338-1082

2. Instrument Description

2.1 Optical Design

The optical design of WFC3 was driven by the need to provide a large field of view and high sensitivity over a broad wavelength range, excellent spatial resolution, and stable and accurate photometric performance. WFC3 features two independent imaging cameras, the UV/optical channel (UVIS) and the near-infrared channel (IR). Figure 1 shows a schematic diagram of the instrument's optical layout. The UVIS channel uses two butted 4096×2051 thinned, back-illuminated Marconi CCD detectors to support imaging between 200 and 1000 nm. The IR channel uses a 1024×1024 Rockwell HgCdTe detector array, with 1014×1014 pixels useful for imaging, to cover the near-infrared between 900 and 1700 nm. A flat

pick-off mirror redirects the on-axis beam coming from the *HST* Optical Telescope Assembly (OTA) into the WFC3. A channel-select mirror inside WFC3 then diverts the light to the IR channel via a fold mirror, or can be removed from the beam to allow light to enter the UVIS channel. Optical elements in each channel correct for the spherical aberration of the *HST* primary mirror. Both channels also have internal flat field illumination sources.

The primary characteristics of the two channels are summarized in Table 1.

Table 1: Characteristics of the two WFC3 channels

Channel	*f*-ratio	Spectral range (nm)	Detector pixel format	Pixel scale (arcsec)	Field of View (arcsec)
UVIS	31	200-1000	2×4096×2051	0.040×0.040	163×164
IR	11	900-1700	1014×1014	0.121×0.135	123×137

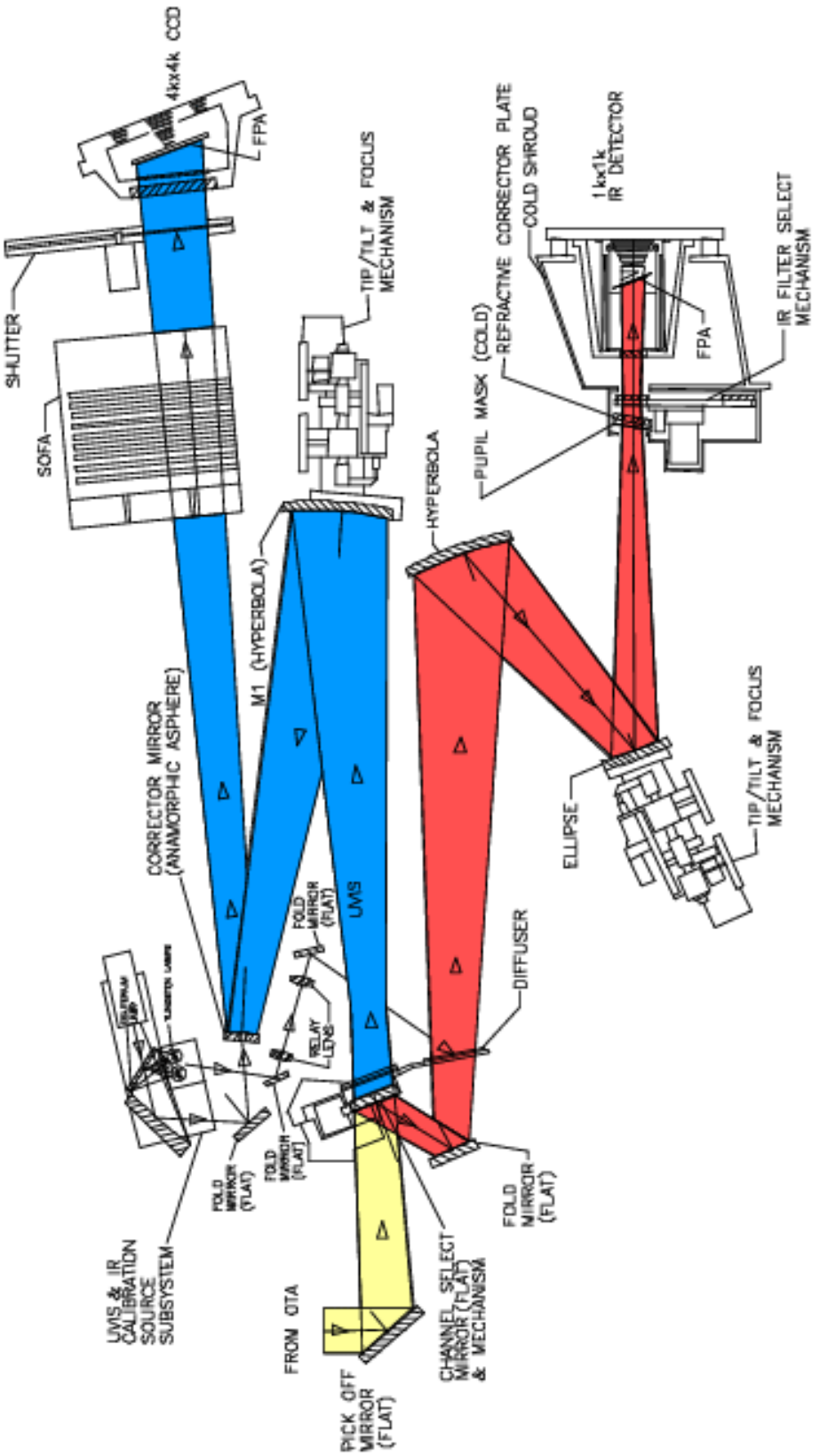

Figure 1: Schematic optical layout of the WFC3 instrument. Yellow indicates light from the OTA, which is sent into the camera by the pick-off mirror. The Channel Select Mechanism then either allows light to pass into the UVIS channel (indicated by the blue path), or directs light into the IR channel (red path). Mechanisms and optics in both channels allow for focus and alignment, and correct for the OTA spherical aberration. Filters and grisms are contained in the UVIS SOFA and the IR FSM. The UVIS channel has a mechanical shutter, while the IR channel is shuttered electronically by the detector. Light is detected by either the UVIS CCDs or the IR focal-plane array. A separate subsystem provides flat field illumination for both channels.

2.2 Field of View and Geometric Distortions

WFC3 will replace WFPC2, *Hubble*'s first large-area camera that included corrections for the spherical aberration of the *HST* primary mirror. The appearance of the *HST* focal plane following a fully successful SM4 is shown in Figure 2.

Figure 2: The *HST* focal-plane layout, showing the instrument complement following a successful SM4. WFC3 will be located on-axis. Outlines of its UVIS and IR channels are shown; they view nearly the same region of the sky, but not simultaneously. The diameter of the outer black circle, projected onto the sky, is about 28 arcminutes.

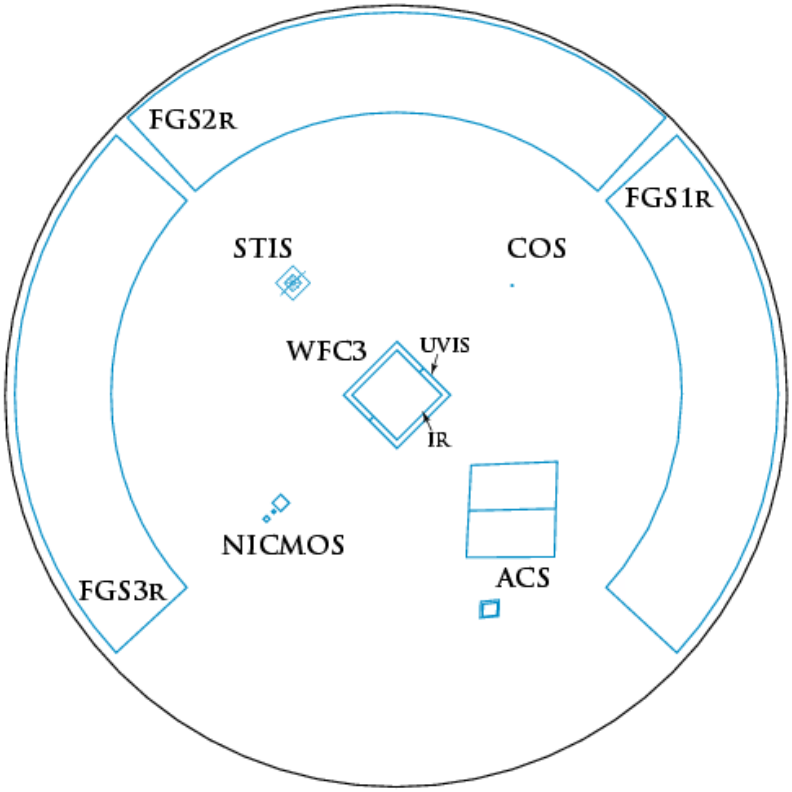

As is the case for ACS, WFC3 images will be subject to significant geometric distortions. These result primarily from the tilt of the focal plane relative to the optical axis (required for constant focus across the detectors; see Figure 1), which leads to a modest elongation of the field of view in both channels. In the UVIS detector, most of the distortion runs approximately parallel to the diagonal direction of the CCD, while it is parallel to the sides of the detector in the IR channel. As a result, the UVIS field projected onto the sky is shaped like a rhombus, with an acute angle between the *x* and *y* axes of the detector of approximately 86 degrees. The IR channel projected onto the sky will be rectangular, with an aspect ratio of about 0.90.

2.3 Spectral Elements

Both WFC3 channels are complemented with a broad selection of spectral elements, chosen on recommendation of the SOC following a Filter Selection Workshop held at STScI on July 14, 1999. The assortment includes broad-, medium-, and narrow-band filters, as well as low-dispersion grisms (one in the UVIS channel, two in the IR channel) for slitless spectroscopy. The broad- and medium-band filters include most of the popular passbands used in extragalactic, stellar, and solar-system astronomy, as well as passbands similar to those already used in other *HST* instruments for photometric consistency and continuity. The classical *UBVRIJH*, Strömgren, and Washington systems are reproduced, along with the filters of the Sloan Digital Sky Survey (SDSS). In addition, several extremely broad-band filters have been included in both channels, for ultra-deep imaging.

There is also a total of 36 different narrow-band passbands in the UVIS channel, consisting of 16 full-field filters and 5 quad filters. (Quad filters are 2×2 mosaics occupying a single filter slot; each one provides four different bandpasses, at the cost of each one covering only about 1/6 of the field of view.) The narrow-band filters provide the capability for high-resolution emission-line imaging in many of the astrophysically important transitions, as well as the methane absorption bands seen in planets, cool stars, and brown dwarfs.

In addition to the broad-band filters, the IR channel includes six narrow-band filters, which likewise sample the most important planetary, stellar, and nebular spectral features in the near-IR.

Finally, broad-band filters with similar wavelength coverages to those of the grism dispersers are available, allowing direct images of spectroscopic targets in the same spectral regions; such images allow accurate identification of the sources as well as providing wavelength calibration.

Unlike ACS or WFPC2, no ramp filters, polarizers, or coronagraphic capabilities are included in either WFC3 channel.

Detailed information about the filters is given in Section 5.2, and Tables 4 and 5 list specifications of the spectral elements of the UVIS and IR channels, respectively, sub-divided by types.

2.4 Detector Read-Out Modes and Dithering

The detectors in both channels offer readouts of subarrays, and the UVIS channel also allows on-chip binning. A variety of dithering schemes will be offered to observers by the Astronomer's Proposal Tool (APT) proposal software, including specially designed "canned" patterns as well as user-defined ones. The post-observation pipeline software will carry out calibration of data taken in all of these configurations, and will offer the

option of reconstructing dithered images with a drizzling algorithm. If the dither pattern incorporates non-integer pixel offsets, it effectively improves the sampling of the point-spread function (PSF). The software will also handle mosaicked images according to a set of rules or associations, and will rectify them onto a cartesian pixel coordinate system.

2.5 Comparison with other *HST* Imaging Instruments

Wavelength Coverage

The WFC3 UVIS channel is similar in design to the Wide Field Channel (WFC) of the ACS. There are, however, a few differences. While ACS/WFC is blind at wavelengths shorter than about 370 nm (i.e., shortward of the *B* band), WFC3/UVIS has sensitivity extending down to 200 nm. The design trade-offs adopted to achieve this extended UV wavelength coverage (primarily the CCD coating and the use of aluminum coatings for the reflective optics; see Figure 1) lead to a reduced sensitivity of WFC3 at longer optical wavelengths compared to that of ACS/WFC.

The ACS does have UV sensitivity in its High Resolution Channel (HRC). However, compared to ACS/HRC, WFC3/UVIS has a factor of 2 higher throughput at the *U* band (see Figure 4 below), and a field of view 35 times the area (but with spatial sampling that is 50% coarser). WFC3/UVIS has no sensitivity in the far-UV region below 200 nm. The far-UV is covered by the ACS Solar-Blind Channel (SBC) and, potentially, by the Space Telescope Imaging Spectrograph (STIS) FUV-MAMA, which may be restored to use during SM4.

The WFC3 IR channel also provides nearly a factor of 2 improvement in sensitivity over NICMOS. However, its wavelength coverage is shorter, ending at about 1700 nm (compared with 2500 nm for NICMOS). The WFC3/IR cutoff at 1700 nm greatly reduces the instrument's sensitivity to the thermal background. Unlike NICMOS, the WFC3 IR channel does not have a cryogenic dewar for cooling of instrument components; instead, all optical components of the IR channel are actively cooled by a thermal-control subsystem. Although much simpler than the NICMOS cryocooler, this design allows the IR detector to be cooled only to ~145 K, and thus does not provide adequate suppression of the thermal background at wavelengths longer than ~1700 nm.

Field of View

Figure 3 schematically illustrates the fields of view (FOVs), on the same scale, for all of the *HST* imaging instruments that will be available following a fully successful SM4.

Figure 3: Schematic diagram comparing relative sizes of the fields of view (FOVs) for all *HST* imaging instruments, following a completely successful SM4. Successive lines of text underneath each FOV give the size in pixels, the pixel scale in arcseconds, and the FOV size in arcseconds. The diagram is schematic, and does not illustrate geometric distortions nor the relative locations in the *HST* focal plane.

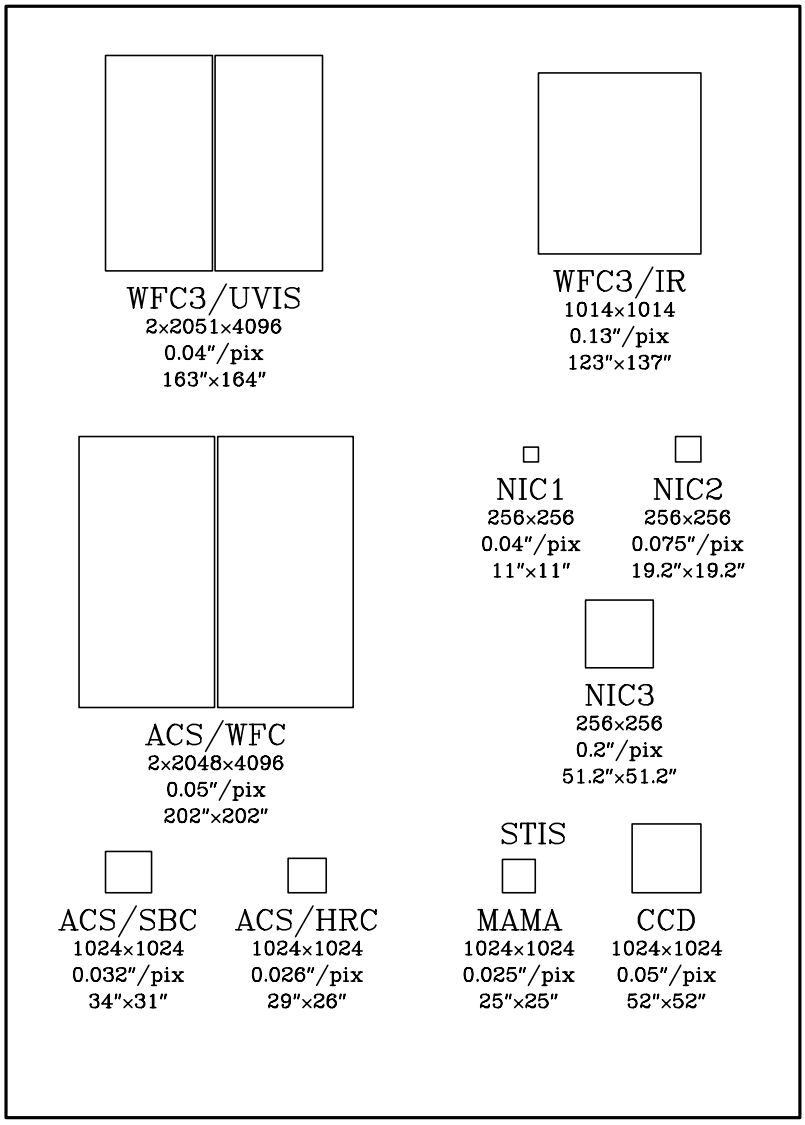

The WFC3 UVIS channel provides about 20% linearly finer pixels than ACS/WFC, obtained at the cost of covering only about 66% of the area of the latter's field of view.

The WFC3 IR channel covers about 6.4 times the area of the NICMOS NIC3 channel, with almost 2 times better spatial sampling, but it lacks the very high spatial samplings offered by the NICMOS/NIC1 and NIC2 channels.

Table 2 presents a comparison of the wavelength coverage, pixel scale, and FOV of WFC3 and of the other *HST* imaging instruments that will be available following a successful SM4. The table includes the imaging characteristics of STIS, which, however, has been disabled since August 2004.

Table 2: Comparison of wavelength coverage, pixel scales, and fields of view of *HST*'s imaging instruments after a successful SM4.

Instrument	Wavelength coverage (nm)	Pixel size (arcsec)	Field of View (arcsec)
WFC3 UVIS	**200 – 1100**	**0.04**	**163×164**
ACS WFC	370 – 1100	0.05	202×202
ACS HRC	200 – 1010	0.025	29×26
ACS SBC	115 – 170	0.03	34×31
STIS FUV-MAMA	115 – 170	0.024	25×25
STIS NUV-MAMA	160 – 310	0.024	25×25
STIS CCD	200 – 1100	0.05	52×52
WFC3 IR	**900 – 1700**	**0.13**	**123×137**
NICMOS NIC1	850 – 2500	0.043	11×11
NICMOS NIC2	850 – 2500	0.075	19×19
NICMOS NIC3	850 – 2500	0.20	51×51

Detector Performance

The UVIS and IR detectors are anticipated to have excellent performance in terms of read-out noise and dark current.

Table 3 summarizes these properties for the WFC3 flight CCD detector and the flight candidate FPA 129 IR detector, and compares them with these parameters for other *HST* imaging detectors that will be available following a successful SM4.

See Table 6 on page 32 for estimates of the limiting magnitudes for WFC3 exposures at UV, optical, and near-IR wavelengths.

Table 3: Characteristics of *HST* imaging detectors available after SM4. Values for the WFC3 detectors are for the flight CCD and flight candidate IR detector FPA 129. The WFC3/IR dark current includes the instrument thermal background.

Detector	Read-out noise, e^- rms	Dark current, e^-/pix/s
WFC3/UVIS	**3.1**	**<0.00014**
ACS/WFC	5.0	0.0038
ACS/HRC	4.7	0.0044
STIS/CCD	5.4	0.004
WFC3/IR	**16**	**<0.4**
NICMOS/NIC2	26	0.3
NICMOS/NIC3	29	0.3

System Throughputs and Discovery Efficiencies

Figure 4 plots the expected system throughputs of the two WFC3 channels as functions of wavelength, compared to those of ACS, NICMOS, and WFPC2. These curves include the throughput of the OTA, all of the optical elements of the instruments themselves, and the sensitivities of the detectors. Throughputs were calculated at the central wavelength (the "pivot wavelength"; see footnote 3 to Table 4 on page 29) of each broad-band filter of each instrument. The WFC3 throughputs are based on the currently selected flight detectors, and are still subject to change at this writing based on further laboratory measurements and the final IR detector choice.

As Figure 4 shows, WFC3 will offer a unique combination of high sensitivity and wide spectral coverage ranging from the UV to the near-IR. WFC3 extends and complements, over a large field of view, the optical performance of ACS/WFC at wavelengths shorter than ~400 nm and longer than 1000 nm. The good degree of functional redundancy with ACS and NICMOS will help ensure that the unique scientific capabilities of *HST* will remain available until the end of its mission.

Another quantity that is useful when comparing different instruments, especially in the context of wide-angle surveys, is the "discovery efficiency," defined as system throughput times area of the FOV as projected onto the sky. In Figure 5 we plot the discovery efficiencies of the *HST* imaging instruments, again vs. wavelength. Note that the *y*-axis is now logarithmic. This figure dramatically illustrates the enormous gains that WFC3 will offer, compared to the current *HST* instruments, both in the optical/UV below 400 nm, and in the near-IR.

Figure 4: System throughputs of imaging instruments on *HST* as functions of wavelength. The plotted quantities are end-to-end throughputs, including filter transmissions, calculated at the pivot wavelength of each broad-band filter of each camera. Throughputs for WFC3 are estimated based on the best information currently available.

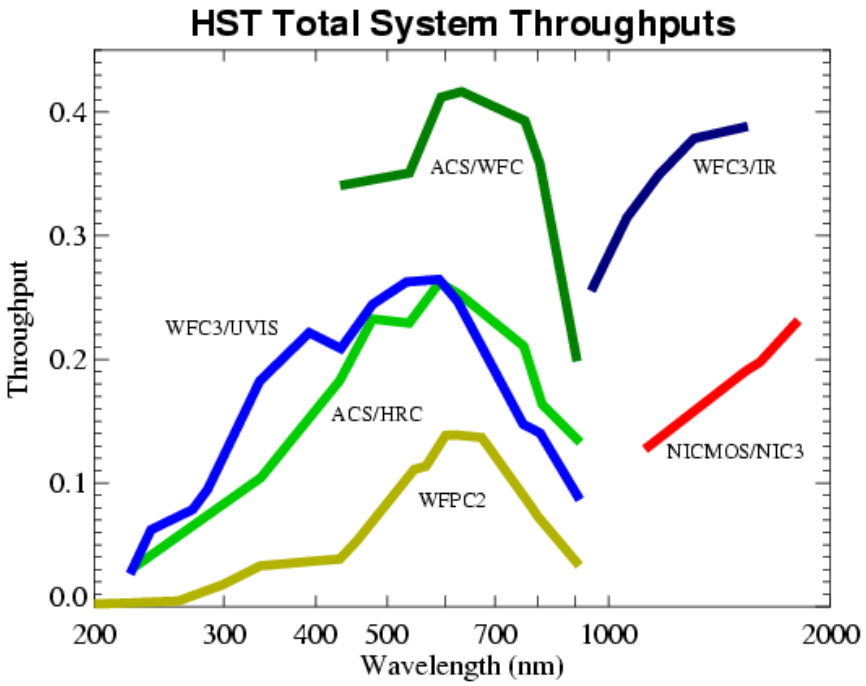

Figure 5: Discovery efficiencies of *HST* imaging instruments, including those expected for WFC3. Discovery efficiency is defined as the system throughput (plotted in Figure 4) multiplied by the area of the field of view. Note that the y-axis is now logarithmic.

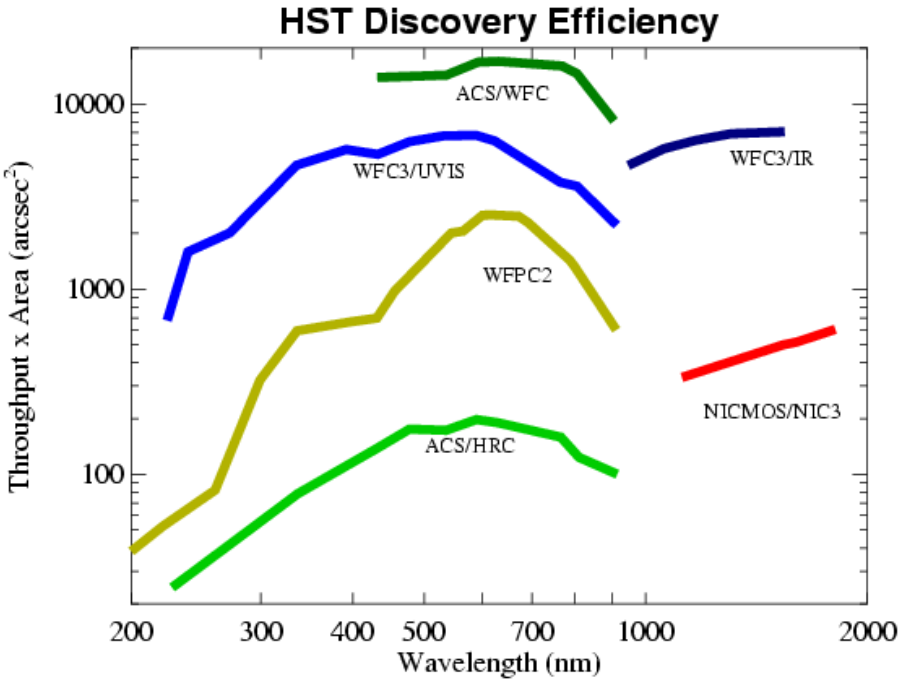

3. The UVIS Channel

The UVIS channel is optimized for highest performance in the 200–400 nm wavelength range. In concept and functionality, as well as in many design details, the UVIS channel is patterned after the ACS/WFC channel. The UVIS channel contains an optical train providing focus and alignment adjustments as well as correction for the OTA spherical aberration, a filter selection mechanism, a shutter mechanism, and a CCD detector assembly. These are supported by a thermal-control subsystem and also by control and data-handling electronics subsystems.

3.1 Field of View and Pixel Size

The field of view of WFC3 is limited by the size of the ~45 degree pick-off mirror (POM), which must be small enough to avoid vignetting of the other off-axis *HST* scientific instruments. The UVIS channel detector adopts the same ACS/WFC camera-head design, with 4096×4102 pixels in the focal plane. The projected pixel shape is not perfectly square due to the geometric distortions discussed in Section 2.2, and the average values of the *x* and *y* scales across the field of view are 0.0397 and 0.0395 arcsec/pixel, yielding a field of view of 163×162 arcsec.

3.2 CCD Detector

The UVIS channel detectors are two 4096×2051 pixel CCDs, butted together to yield a total 4096×4102 array with a gap between the two chips of approximately 50 pixels (2 arcsec). The gap can be filled in final images, when desired, by using appropriate dithering strategies. The CCDs are thinned, back-illuminated Marconi Corporation (now e2v technologies Ltd.) devices with UV-optimized anti-reflection coatings and 15 μm pixels. As shown in Figure 2, the CCD sensitivity extends down to 200 nm, while remaining relatively high at visible and near-IR wavelengths. The UVIS channel optics are UV-optimized, with high throughput in the 200-350 nm range achieved by employing aluminized mirrors with magnesium fluoride (MgF_2) coatings.

Although highly optimized for the UV, this design works reasonably well out into the red part of the spectrum too, yielding a reflectivity of ~88%. The overall system throughput of WFC3 in the *R* band is ~50% that of ACS/WFC.

Detector readout noise is expected to be 3.1 electrons rms, and the dark current less than 0.5 electrons per pixel per hour. Such low values allow background-limited observations in broad-band filters at visible and longer wavelengths in single one-orbit-long exposures.

Accurate photometric performance requires uniform response within each pixel and excellent charge-transfer efficiency (CTE), which must be stable over a relatively long lifetime in the high-radiation environment in which *HST* operates. The non-optimal CTE characteristics of the WFPC2 CCDs at launch, and their further degradation on orbit, have significantly limited high-accuracy photometry. The anticipated performance of the WFC3 CCD detectors has been improved by providing shielding to the CCDs (same as ACS/WFC and similar to WFPC2) and designing the CCDs with a mini-channel (improved over ACS/WFC), which will reduce the number of traps seen by small charge packets during transfers. In addition, WFC3 is the first *HST* instrument with the option of charge injection, which can mitigate the effects of CTE losses. In the later years, this option can be activated to fill in charge traps, without an excessive increase in the noise level of the images.

Another important detector parameter is the modulation transfer function (MTF), which defines how accurately a detector responds to a scene with high-spatial-frequency structure. MTF performance decreases with increasingly non-uniform response within a pixel (which determines the potential photometric accuracy), and with increasing cross-talk between pixels (which degrades PSF sharpness). Measured limits to the MTF of the UVIS CCDs imply less than 10% degradation of the PSF width over the whole spectral range, and a capability to do better than 2% photometry in the visible.

3.3 Spectral Elements

The UVIS channel makes use of the refurbished WF/PC1 Selectable Optical Filter Assembly (SOFA) unit. The SOFA contains 12 filter wheels, each one accommodating four spectral elements along with an open position, making a total of 48 slots available for filters or grisms. These slots have been populated with 42 narrow-, medium-, and broad-band filters, one UV grism, and 5 quad filters (each one containing 4 individual filters in a 2×2 mosaic configuration), bringing the total to 63 individual spectral elements.

Table 4 on page 29 lists the available UVIS spectral elements. They include several very broad-band filters for extremely deep imaging; filters that match the most commonly used filters on WFPC2 (to provide continuity with previous observations); the SDSS filters; and filters that are optimized to provide maximum sensitivity to various stellar parameters (e.g., the Strömgren and Washington systems, and the F300X filter for high sensitivity to the stellar Balmer jump). There is also a wide array of narrow-band filters, which will allow investigations of a range of physical conditions in the interstellar medium, nebulae, and solar system. A few of the narrow-band filters are also provided with slightly redshifted wavelengths, for use in extragalactic applications.

The UV grism, G280, will provide slitless spectra with a dispersion of about 1.4 nm/pix, or a 2-pixel resolving power of about R=125. These spectra cover the approximate spectral range 200-500 nm.

In most cases, a grism observation will be accompanied by a direct image, for source identification and wavelength calibration. A suitable filter for this purpose is F200LP.

3.4 Operating Modes

The UVIS channel's only observing mode offered to General Observers (GOs) is called "ACCUM," a configuration in which photons are counted on the CCD detectors as accumulated charge after an initial reset. The minimum exposure time is 0.5 s. The charge is read out at the end of an exposure, converted to Data Numbers (DN) at a pre-defined gain (1.5 e^-/DN), stored in a data memory array, and, when the array is full, dumped to the science data recorder onboard *HST*.

In addition to a full-array image, the user can request subarray or on-chip binned images. A suite of fixed, pre-defined subarray apertures will be available to GOs, as well as a limited capability for user-defined subarrays. The subarray option may be used to minimize data volume and read-out time, in situations where it is scientifically acceptable to reduce the size of the field of view. Examples include observations of bright point sources or small fields, solar-system objects, or time-series monitoring of rapidly varying objects.

The on-chip binning option, with choices of 2×2 or 3×3, allows for better sensitivity in cases of low-background observations (e.g., narrow-band and/or UV imaging). Binning can reduce the contribution from CCD read-out noise, when maximum spatial resolution is of secondary importance. Binning will also reduce data volume. However, it will increase the fraction of pixels impacted by cosmic-ray hits.

GOs will be able to select from among a suite of standard dithering patterns, including both integer and fractional-pixel shifts, obtained by moving the telescope. (Note, however, that integer pixel shifts can effectively take place only over relatively small portions of the field of view because of geometric distortions.) The fractional-pixel patterns will help improve the effective resolution by allowing the user to improve the sampling of the PSF by suitable combination of the dithered images (drizzling), while at the same time minimizing the effects of detector cosmetic defects. Dither patterns will also be offered for the purpose of filling in the gap between the two CCD chips.

4. The IR Channel

The IR Channel is optimized over the wavelength range 900-1700 nm. The IR optics, with the exception of the WFC3 pick-off mirror (which intercepts the central bundle of light from the OTA and is shared with the UVIS channel), are coated with a protected silver layer for maximum IR throughput. The IR channel consists of the following components: (a) the Channel Select Mechanism (CSM), which diverts light from the UVIS channel optical train; (b) a two-mirror mechanism providing focus and alignment adjustments; (c) a lens (the Refractive Corrector Plate or RCP) for spherical-aberration correction; (d) the Filter Selection Mechanism (FSM); and finally (e) the HgCdTe IR detector assembly inside a vacuum enclosure sealed by a transparent window. The IR optical chain is supported by a thermal control subsystem and also by control and data-handling electronics subsystems. Because the detector is electronically shuttered, a mechanical shutter is not needed; bright-object protection when the IR channel is not in use is obtained by blocking the optical path with an opaque slot in the FSM.

4.1 Field of View and Pixel Size

The pixel size for the IR detector, as projected onto the sky, was selected by the SOC and Science IPT after careful analysis; it achieves an optimal balance between size of the field of view and PSF sampling. Simulations showed that dithering and image-reconstruction techniques would be able to reconstruct a good-quality PSF satisfactorily, as long as the pixel size was below 0.15 arcsec. The final choice of ~0.13×0.13 arcsec satisfies this requirement, while at the same time conforming to optical packaging considerations. Because the focal plane is tilted by about 22 degrees with respect to the beam, the field of view is rectangular in shape, with an aspect ratio of ~0.90. The scale of the rectangular pixels is 0.121×0.135 arcsec, yielding a useful field of view of 123×137 arcsec.

4.2 IR Detector Array

The WFC3 IR detector is a Rockwell HgCdTe 1024×1024 array with 18 μm pixels, bonded onto a silicon multiplexer (MUX). The inner 1014×1014 pixels are light-sensitive and are used for scientific imaging, while the bordering 5 pixels around the array edges provide a constant-voltage reference and are used for improved subtraction of the electronic bias level. This device is a direct descendant of the NICMOS 256×256 and Hawaii 1024×1024 arrays, widely used in space- and ground-based astronomy. A

major effort has been made to eliminate the amplifier glow and bias jumps that have affected the NICMOS detectors.

To avoid the complexity and limited lifetime of a stored-cryogen system, while at the same time provide the low operating temperatures required for dark-current and thermal-background reduction, the WFC3 IR detector is refrigerated with a six-stage thermoelectric cooler to a nominal operating temperature of 145 K. The long-wavelength cutoff at 1700 nm (provided by tailoring the composition of the HgCdTe array) has been chosen to limit the "effective" dark current (i.e., the sum of the intrinsic detector dark current and the instrument's internal thermal background), given the restrictions imposed by the operating temperature. A longer cutoff wavelength would have increased the effective dark current at a given detector operating temperature, because of the thermal background from the telescope and optical bench.

The currently selected candidate flight detector (FPA 129) has a read-out noise of about 16 electrons rms per pixel after multiple reads. The sum of detector dark current and thermal background contributions is predicted to be lower than the requirement of 0.4 electrons per pixel per second.

The MTF of the IR detector is not expected to broaden the PSF by more than 10%. The intrinsic photometric accuracy is expected to be better than 5%.

4.3 Internal and OTA Thermal Background

Given the overall design of the IR channel, particular care has been put into minimizing the thermal background contribution to the detector effective dark current and into reducing the thermal load on the detector. This has been achieved by cooling the optical bench, by designing a cooled, baffled camera head for the IR detector, and by including a cold-stop mask in the design. This latter component greatly decreases both the thermal load and the effective background coming from the instrument itself and from the *HST* OTA, meeting the goal of 0.2 electrons/pixel/s in the *"H"* (F160W) band, at the cost of a modest throughput loss of ~10%. Because the contribution to the background by zodiacal light is ~0.2 electrons/pixel/s in the F160W band, the instrument will meet a goal of being near-background-limited in this passband. Similar performance is achieved in the F125W band. The IR channel filter wheel is also cooled to reduce its contribution to the background, due to the off-band emissivity of the filters.

4.4 Spectral Elements

The IR channel's FSM contains a single filter wheel with 18 slots, containing 15 passband filters, two grisms, and an opaque blank position.

The filter complement, as recommended by the SOC with community input, samples the range from 900 to 1700 nm. It includes broad- and medium-band filters covering the entire range, as well as several filters centered on molecular bands and nearby continua. There are also several narrow-band filters probing interstellar and nebular diagnostic lines. Table 5 on page 31 lists the names and characteristics of the IR spectral elements.

The IR channel's versions of the ground-based *J* and *H* filters are F125W and F160W, respectively. The F125W filter has a width somewhat wider than that of a typical *J* passband used in ground-based cameras. The F160W filter's bandpass has been blue-shifted relative to ground-based *H* in order to give a better fit to the quantum-efficiency curve of the IR detector. Specifically, the *H* bandpass has been narrowed to approximately 1400-1700 nm, in order to limit thermal background, and to have the filter transmission define the bandpass at the red end rather than the detector sensitivity cutoff. By contrast, the NICMOS *H* filter (NICMOS F160W) covers approximately 1400-1800 nm. This narrowing for WFC3 minimizes photometric errors due to spatial variations in the detector's sensitivity function.

The wide F140W filter covers the gap between the *J* and *H* bands that is inaccessible from the ground. F105W has a central wavelength similar to ground-based *Y*, but is considerably wider. The IR channel also includes a very wide filter, F110W, spanning the ground-based *Y* and *J* bands. This filter can be used for deep imaging, with a bandpass fairly similar to that of the corresponding broad-band filter (also called F110W) in NICMOS. .

The two grisms will provide the WFC3 IR channel with the ability to obtain slitless spectra. The "blue" G102 grism provides a dispersion of 2.5 nm/pix (or a 2-pixel resolving power of ~200) over the 900-1150 nm wavelength range. The "red" G141 grism has a dispersion of 4.9 nm/pix (resolving power of ~140) over the 1080-1700 nm range. These dispersions and resolving powers are still only predicted values at this writing, pending laboratory measurements.

In most cases, a grism observation will be accompanied by a direct image, for source identification and wavelength calibration. Recommended filters for this purpose are F098M for the G102 grism, and F140W for G141.

4.5 Operating Modes

The standard operating mode for the IR channel, "MULTIACCUM," begins with an array reset followed by one or more non-destructive readouts as the exposure charge accumulates. The number of readouts (up to 15 after the initial reset) can be requested by the observer, and all readouts are recorded and transmitted to the ground for analysis. The

accumulated signal is converted to DN with a gain of 2.5 e^-/DN. The minimum exposure time is 4.3 s.

On-orbit experience with NICMOS shows that non-destructive readout is very effective, because it reduces the effective readout noise and corrects for most cosmic-ray hits. Many IR observations are expected to make use of sub-pixel dithering to improve the PSF sampling. Suitable dithering patterns will be included in the proposal software tools (APT), and can be requested by the observer. The IR channel also supports four subarray readout modes to allow for the short integration times required by bright targets (e.g., standard stars or bright solar-system targets), as well as reduction of data volume. The subarrays are always centered on the detector center, and the available sizes are 64×64, 128×128, 256×256, and 512×512 pixels.

5. Observing with WFC3

This section addresses the general questions that arise when observers choose between planning to use WFC3 in a future observing cycle vs. proposing for an existing imaging instrument for Cycle 16.

To support such decisions, this section also presents detailed specifications for the WFC3 spectral elements, and gives guidance on the anticipated WFC3 performance. There is also a brief discussion of parallel observations (i.e., simultaneous observations with WFC3 and ACS). It must be remembered, however, that these specifications, although as accurate as possible at this writing, are still preliminary and subject to possible changes.

5.1 Choosing the Optimum Scientific Instrument

When facing the decision whether to propose WFC3 observations in a future cycle, or to propose now for other existing scientific instruments, observers should carefully evaluate the capabilities of WFC3 and compare them to those of the other *HST* instruments, in the context of their own scientific goals.

Observers should especially note that WFC3 intentionally provides some redundancy with the ACS and NICMOS instruments, in order to provide some protection against potential failures of either of those instruments. On the other hand, WFC3 also differs sufficiently from those instruments (in fact, it largely complements them). Therefore, observers do need to give careful consideration to instrument capabilities in order to optimize the observations. The primary factors to consider in choosing the best instrument are areal coverage, spatial resolution, wavelength coverage, sensitivity, and availability of specific spectral elements. Table 2 on page

11 lists the primary characteristics of the imaging instruments that will be available on *HST* following a successful SM4.

For some research programs, the instrument choice may be dictated by the need for a particular spectral element. In this regard, WFC3 offers considerable capability because of its broad complement of wide-, medium-, and narrow-band filters both at UV/optical and near-IR wavelengths, as well as one UV grism and two near-IR grisms for slitless spectroscopy. See Table 4 and Table 5 below.

For studies at optical wavelengths, the trade-offs to consider when deciding between WFC3/UVIS and ACS/WFC include pixel size, field of view and, to some extent, throughput. WFC3 is generally preferable when angular resolution has higher priority than field of view, because of its finer pixel size. On the other hand, ACS/WFC has higher throughput than WFC3/UVIS at wavelengths longward of 400 nm (see Figure 4), and hence it should be used if the highest possible sensitivity at such wavelengths is crucial. However, considerations of degraded charge-transfer efficiency (CTE) should also be kept in mind, since ACS will have been in the high-radiation space environment for about six years at the time when WFC3 may come on line.

At UV wavelengths, WFC3/UVIS is the only imager on *HST* to offer a large field of view combined with high throughput. However, its spectral coverage does not extend shortward of 200 nm, whereas ACS/SBC and STIS/FUV-MAMA (if STIS operation is restored during SM4) both reach down to 115 nm (STIS/NUV-MAMA reaches 160 nm), and also offer finer spatial sampling (see Table 2). Thus, WFC3 will be the choice whenever both large field of view and coverage down to 200 nm are required (e.g., multi-wavelength surveys). However, if observations at extreme far-UV wavelengths are necessary, or if the highest available spatial sampling is a primary requirement, then ACS/HRC, ACS/SBC, or the STIS UV channels should be considered.

At near-IR wavelengths WFC3/IR offers a much larger field of view and, generally, higher throughput than NICMOS. It also offers greatly improved sensitivity and ease of data reduction and calibration, due to the accurate bias subtraction made possible by the presence of reference pixels. However, WFC3 sensitivity is limited to wavelengths shortward of ~1700 nm, and WFC3 has coarser pixel sizes than NIC1 and NIC2.

5.2 Specifications for UVIS and IR Spectral Elements

As described above, the spectral elements for WFC3 have been chosen to cover many scientific applications, from color selection of distant galaxies, to accurate photometry of stellar sources and narrow-band imaging of nebular gas. The WFC3 filter suite was defined by the SOC, with input from the astronomical community. To reflect the importance of the blue and ultraviolet wavelength regimes and the high short-wavelength

sensitivity of the WFC3 UVIS channel, several near-UV filters are included in the UVIS filter set. Spanning the entire wavelength region are filters consistent with the WFPC2, ACS, and NICMOS sets, various widely used photometric systems, and the Sloan survey filters. The shape of the passband of some filters has been designed for specific purposes, such as providing maximum throughput (e.g., some of the near-UV filters) or matching the response of the detector to provide photometric accuracy (e.g., the *H* band in the IR channel, as discussed in Section 4.4). Table 4 and Table 5 list the available passbands for the UVIS and IR channels, respectively, and their characteristics.

Figure 6 through Figure 11 present detailed plots of the total system throughput for each of the UVIS and IR filters. The throughput calculations include the quantum efficiencies of the UVIS flight CCD and of the IR flight candidate detector FPA 129.

Figure 6: Integrated system throughput of the WFC3 UVIS long-pass and extremely wide filters (top panel) and of the wide-band filters covering 2000-6000 A (bottom panel). The throughput calculations include the *HST* OTA, WFC3 UVIS-channel internal throughput, filter transmittance, and the QE of the UVIS flight detector. Throughputs in all plots below ~3200 A include correction for quantum yield. Instrument throughput is not yet well-characterized below 2000 A and above 10,000 A.

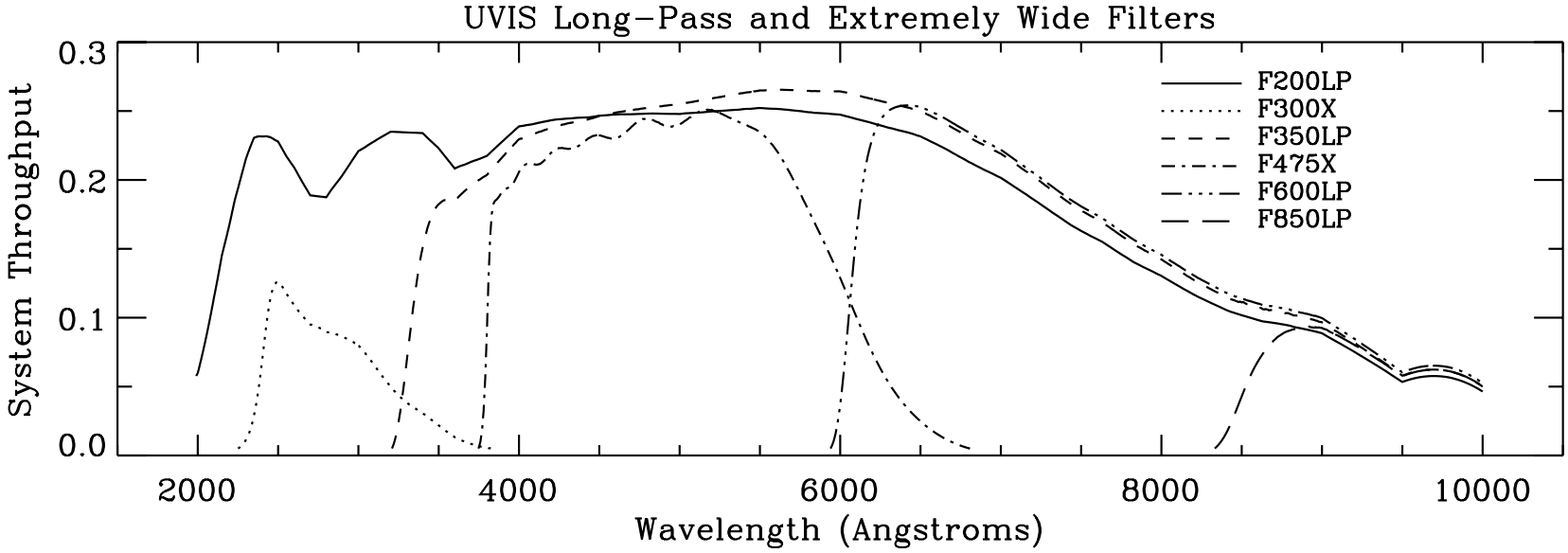

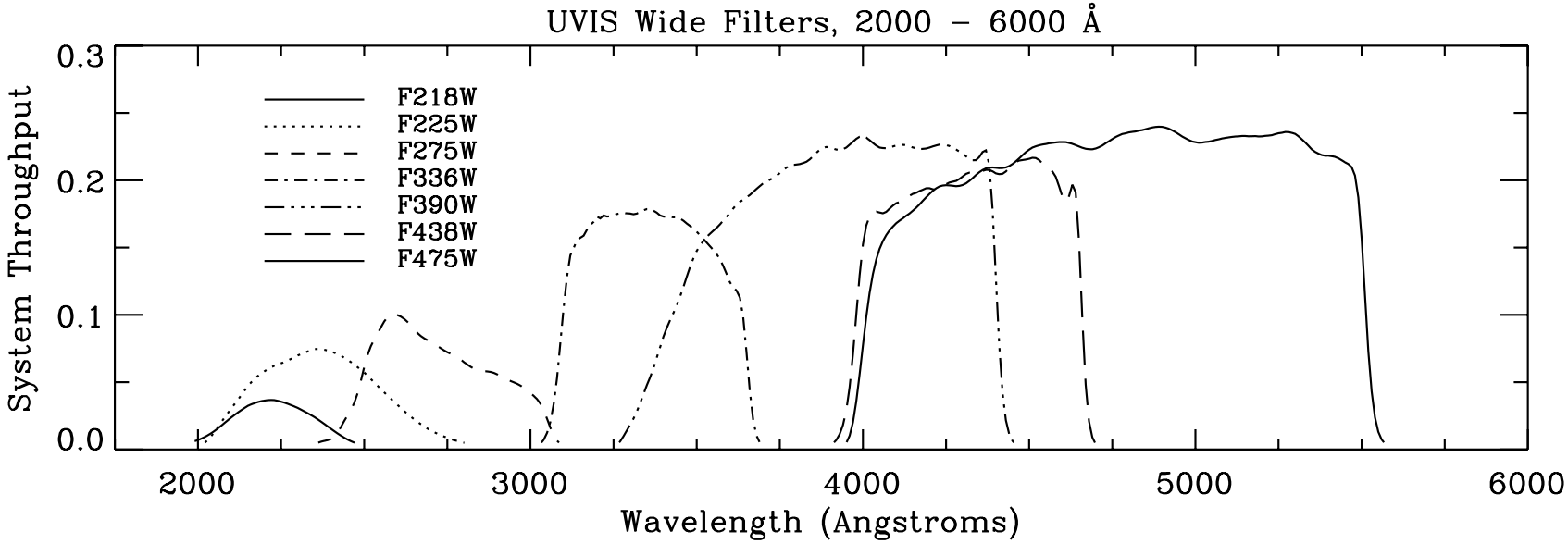

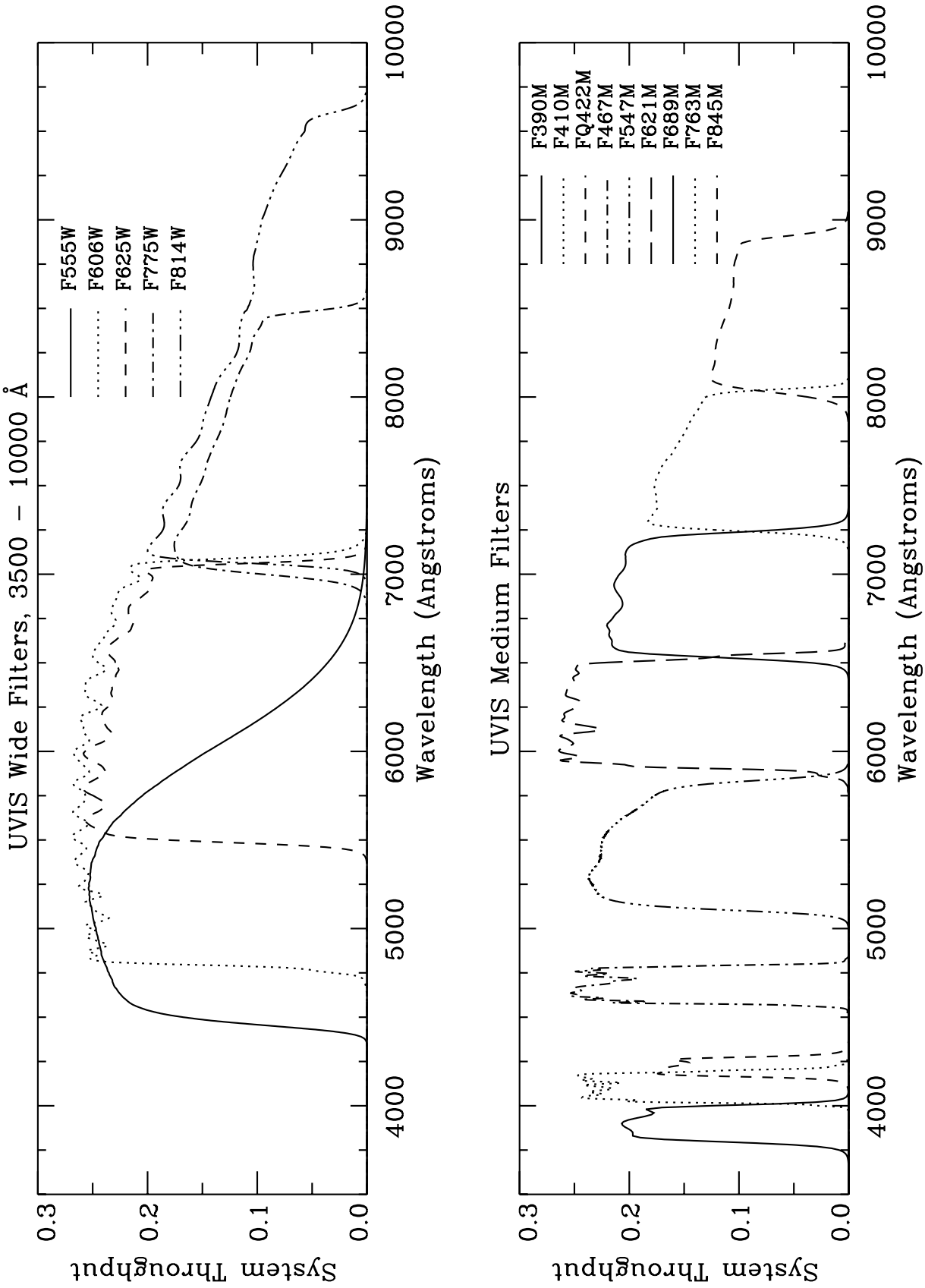

Figure 7: Integrated system throughput of the WFC3 UVIS wide-band filters covering 3500-10,000 A (top panel) and the medium-band filters (bottom panel). The throughput calculations include the *HST* OTA, WFC3 UVIS-channel internal throughput, filter transmittance, and the QE of the UVIS flight detector.

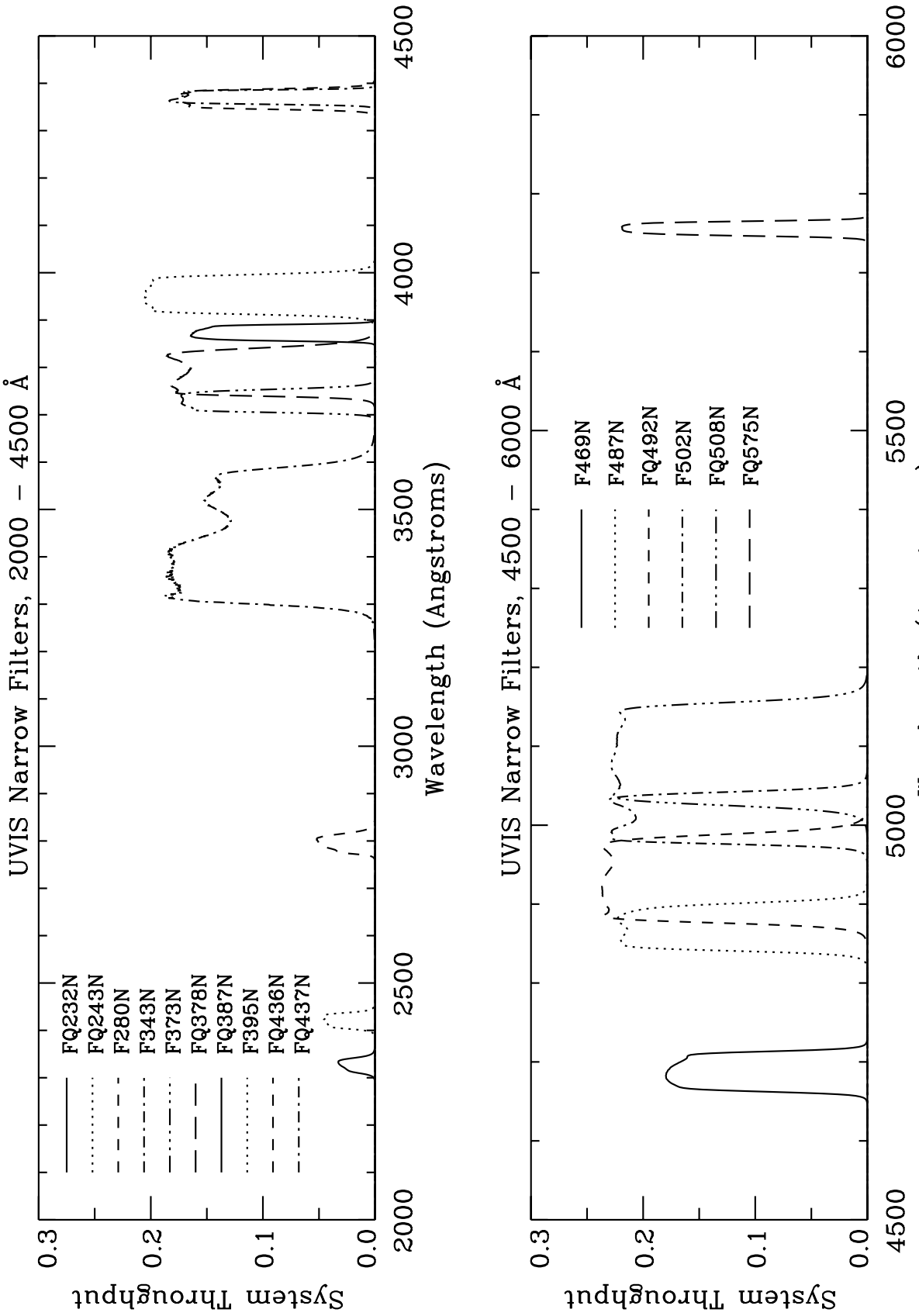

Figure 8: Integrated system throughput of the WFC3 UVIS narrow-band filters covering 2000-4500 A (top panel) and the narrow-band filters covering 4500-6000 A (bottom panel). The throughput calculations include the *HST* OTA, WFC3 UVIS-channel internal throughput, filter transmittance, and the QE of the UVIS flight detector.

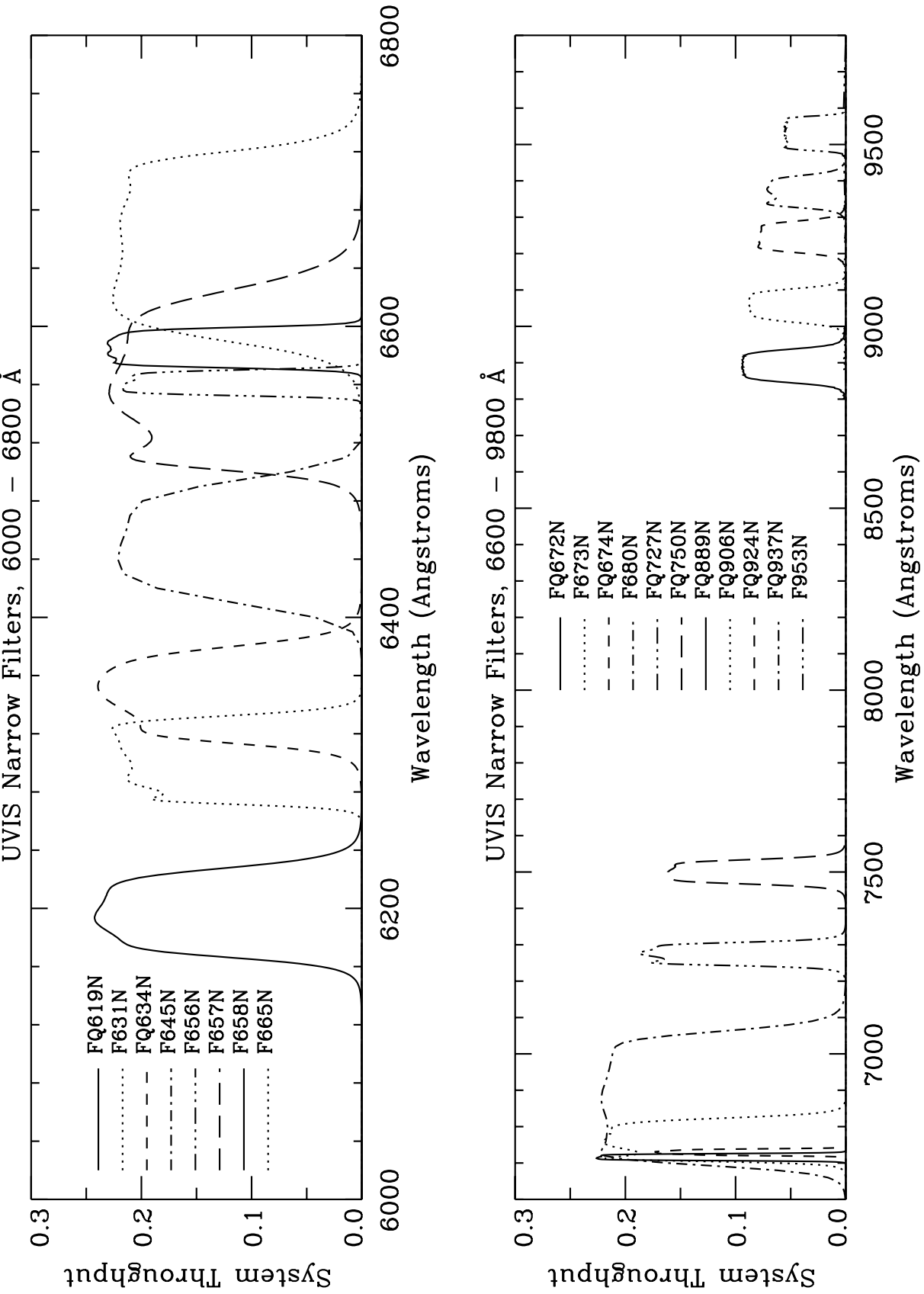

Figure 9: integrated system throughput of the WFC3 UVIS narrow-band filters covering 6000-6800 A (top panel) and the narrow-band filters covering 6600-9800 A (bottom panel). The throughput calculations include the *HST* OTA, WFC3 UVIS-channel internal throughput, filter transmittance, and the QE of the UVIS flight detector.

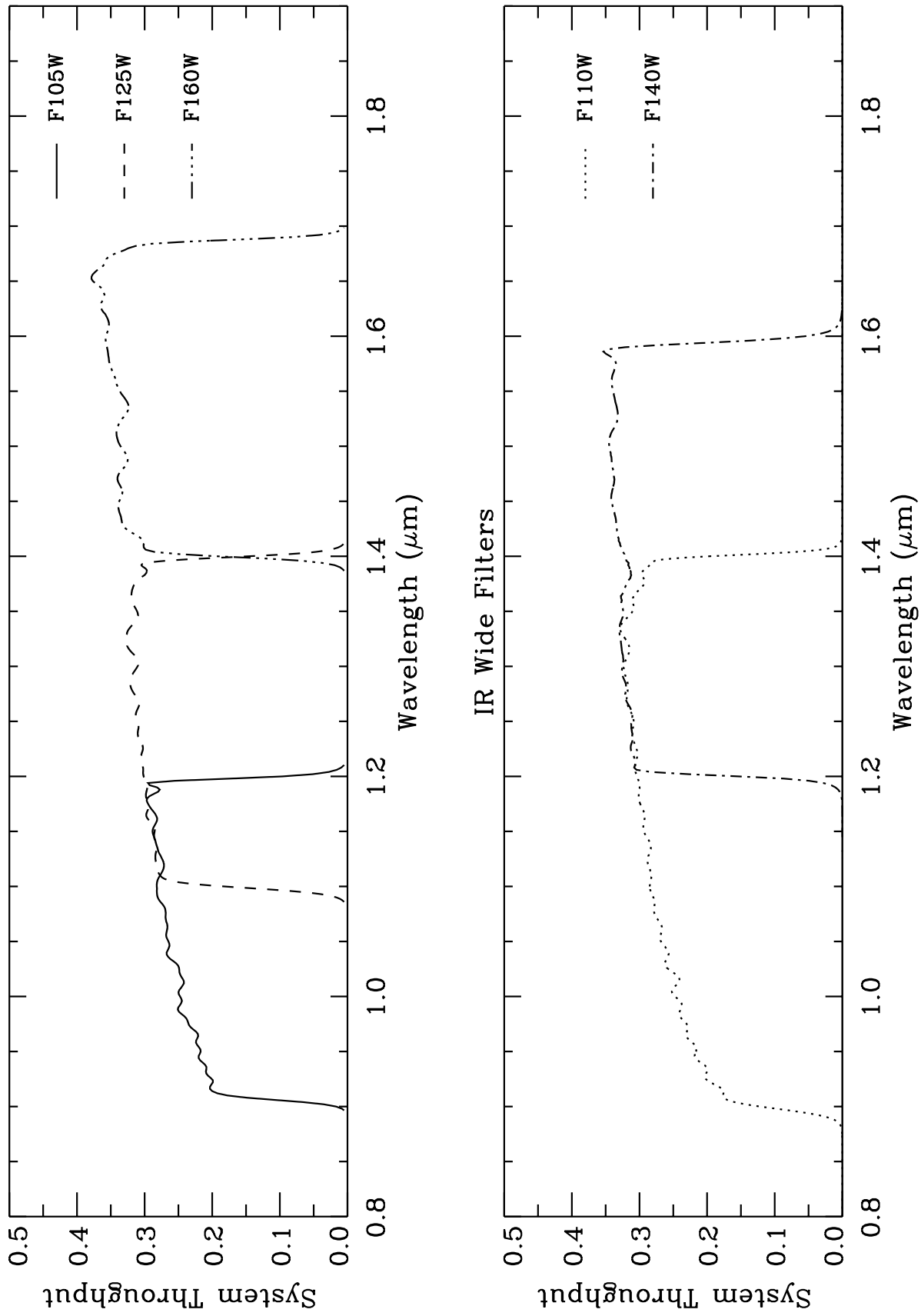

Figure 10: Integrated system throughput of the WFC3 IR wide-band filters, presented in two panels for clarity. The throughput calculations include the *HST* OTA, WFC3 IR-channel internal throughput, filter transmittance, and the QE of the FPA129 flight candidate IR detector.

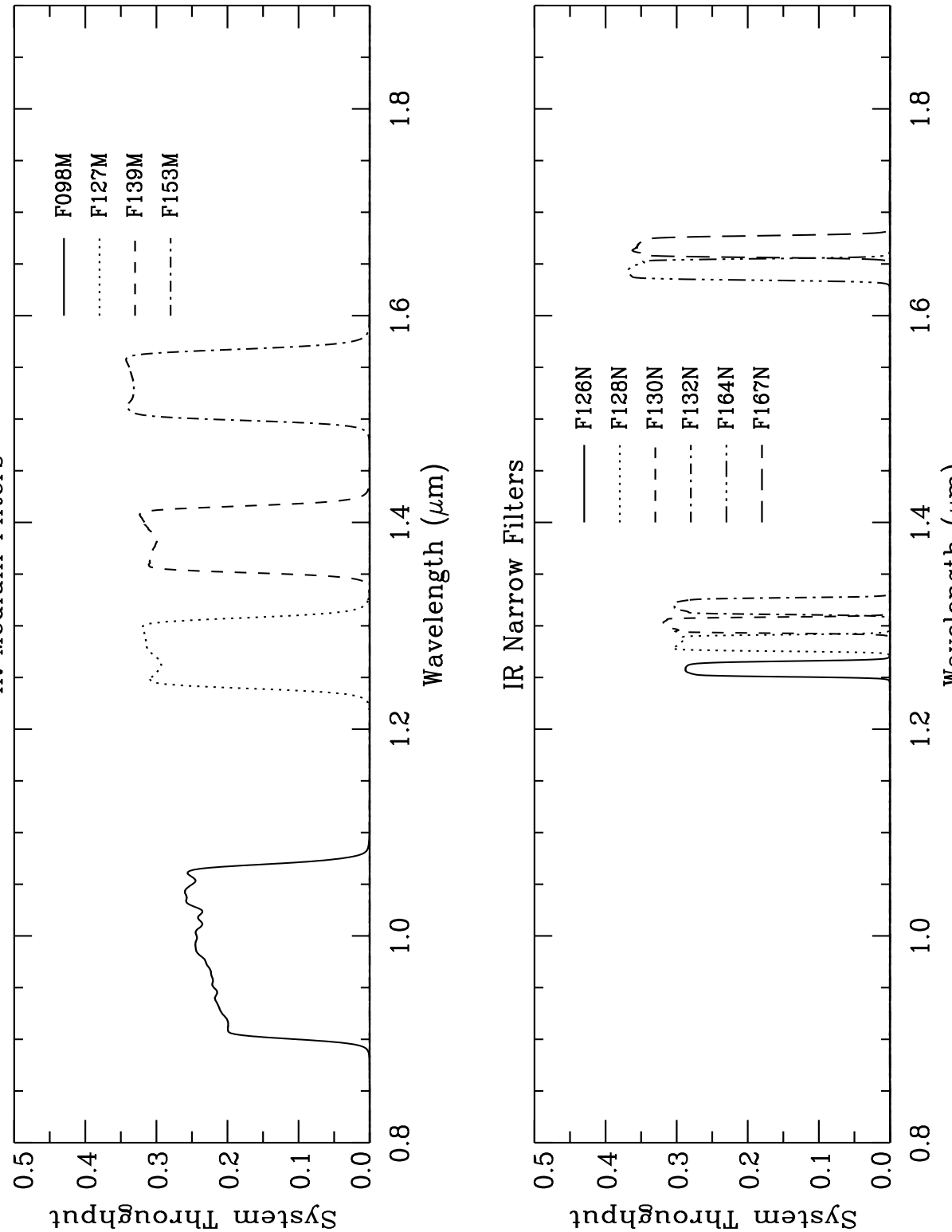

Figure 11: Integrated system throughput of the WFC3 IR medium-band filters (top panel) and narrow-band filters (bottom panel). The throughput calculations include the *HST* OTA, WFC3 IR-channel internal throughput, filter transmittance, and the QE of the FPA129 flight candidate IR detector.

Table 4: WFC3 UVIS Channel Filters and Grism

Name[1]	Description[2]	Pivot[3] λ (Å)	Width[4] (Å)	Peak Transmission
UVIS Long-Pass (LP) and Extremely Wide (X) Filters				
F200LP	Clear; grism reference	5686.9	(6500)	0.98
F300X	Extremely wide UV	2829.8	753.0	0.53
F350LP	Long pass	6812.0	(4500)	0.98
F475X	Extremely wide blue	4917.1	2199.6	0.94
F600LP	Long pass	8430.2	(4000)	0.99
F850LP	SDSS *z*′	9756.4	(1500)	0.96
UVIS Wide-Band (W) Filters				
F218W	ISM feature	2183.0	351.7	0.23
F225W	UV wide	2341.0	547.3	0.32
F275W	UV wide	2715.3	480.8	0.46
F336W	*U*, Strömgren *u*	3361.1	553.8	0.75
F390W	Washington *C*	3904.6	953.0	0.96
F438W	WFPC2 *B*	4318.7	676.8	0.84
F475W	SDSS *g*′	4760.6	1488.9	0.92
F555W	WFPC2 *V*	5309.8	1595.1	0.95
F606W	WFPC2 Wide *V*	5907.0	2304.2	0.99
F625W	SDSS *r*′	6254.0	1575.4	0.95
F775W	SDSS *i*′	7733.6	1486.0	0.85
F814W	WFPC2 Wide *I*	8304.7	2543.3	0.97
UVIS Medium-Band (M) Filters				
F390M	Ca II continuum	3893.8	210.5	0.88
F410M	Strömgren *v*	4107.0	182.8	0.98
FQ422M	Blue continuum	4217.7	113.3	0.69
F467M	Strömgren *b*	4680.7	218.0	0.98
F547M	Strömgren *y*	5447.0	714.0	0.88
F621M	11% passband	6216.7	631.0	0.99
F689M	11% passband	6886.0	708.6	0.94
F763M	11% passband	7636.3	798.6	0.97
F845M	11% passband	8468.9	886.7	0.96
UVIS Narrow-Band (N) Filters				
FQ232N	C II] 2326	2326.9	32.2	0.12
FQ243N	[Ne IV] 2425	2420.6	34.8	0.15
F280N	Mg II 2795/2802	2796.8	22.9	0.27
F343N	[Ne V] 3426	3438.0	140.0	0.78
F373N	[O II] 3726/3728	3729.6	39.2	0.78
FQ378N	*z* ([O II] 3726)	3790.9	89.2	0.83
FQ387N	[Ne III] 3868	3873.0	23.1	0.72
F395N	Ca II 3933/3968	3953.7	72.9	0.86
FQ436N	Hγ 4340 + [O III] 4363	4366.7	35.7	0.67
FQ437N	[O III] 4363	4370.6	24.6	0.70
F469N	He II 4686	4687.5	37.2	0.69
F487N	Hβ 4861	4870.7	48.4	0.85
FQ492N	*z* (Hβ)	4932.1	101.0	0.85

Name[1]	Description[2]	Pivot[3] λ (Å)	Width[4] (Å)	Peak Transmission
	UVIS Narrow-Band (N) Filters (continued)			
F502N	[O III] 5007	5009.0	57.8	0.87
FQ508N	*z* ([O III] 5007)	5089.7	117.9	0.87
FQ575N	[N II] 5754	5755.9	12.9	0.78
FQ619N	CH_4 6194	6197.5	61.6	0.89
F631N	[O I] 6300	6303.0	43.1	0.86
FQ634N	6194 continuum	6347.5	66.2	0.88
F645N	Continuum	6451.6	85.0	0.86
F656N	Hα 6562	6561.1	13.9	0.86
F657N	Wide Hα + [N II]	6565.1	96.3	0.90
F658N	[N II] 6583	6585.2	23.6	0.92
F665N	*z* (Hα + [N II])	6654.4	109.0	0.90
FQ672N	[S II] 6717	6716.1	14.9	0.89
F673N	[S II] 6717/6731	6764.5	100.5	0.91
FQ674N	[S II] 6731	6729.5	10.0	0.68
F680N	*z* (Hα + [N II])	6878.6	323.6	0.95
FQ727N	CH_4 7270	7274.7	64.8	0.89
FQ750N	7270 continuum	7500.6	68.8	0.85
FQ889N	CH_4 25 km-agt[5]	8891.8	93.7	0.90
FQ906N	CH_4 2.5 km-agt	9056.7	94.0	0.92
FQ924N	CH_4 0.25 km-agt	9246.3	89.2	0.94
FQ937N	CH_4 0.025 km-agt	9371.1	91.9	0.91
F953N	[S III] 9532	9529.7	84.6	0.90
	UVIS Grism (G)			
G280	UV grism	(2775)	1850	0.4

1. The spectral-element-naming convention is as follows for both the UVIS and IR channels. All filter names begin with F, and grisms with G; if the filter is part of a four-element quad mosaic, a Q follows F. Then there is a three-digit number giving the nominal effective wavelength of the bandpass, in nm (UVIS channel) or nm/10 (IR channel). (For long-pass filters, the number is instead the nominal blue cutoff wavelength in nm.) Finally, for the filters, one or two letters indicate the bandpass width: X (extremely wide), LP (long pass), W (wide), M (medium), or N (narrow).
2. Filters intended for imaging in a redshifted bandpass are given descriptions similar to the following: "*z* (Hα + [N II])".
3. "Pivot wavelength" is a measure of the effective wavelength of a filter (see A. Tokunaga & W. Vacca 2006, PASP, 117, 421). It is calculated here based only on the filter transmission. Values are approximate for the long-pass filters.
4. Full width at 50% of peak transmission for wide and medium bands, and at 10% of peak transmission for narrow bands. For long-pass filters, the widths are approximate and include convolution with the detector QE.
5. km-agt (km-amagat) is a unit of vertical column density, equal to 2.69×10^{24} molecules/cm^2.

Table 5: WFC3 IR Channel Filters and Grisms

Name[1]	Description	Pivot[2] λ (nm)	Width[3] (nm)	Peak Transmission
	IR Wide-Band (W) Filters			
F105W	Wide *Y*	1048.95	292.30	0.98
F110W	Wide *YJ*	1141.40	503.40	0.99
F125W	Wide *J*	1245.90	301.50	0.98
F140W	Wide *JH* gap; red grism reference	1392.10	399.00	0.99
F160W	Blue-shifted *H*	1540.52	287.88	0.98
	IR Medium-Band (M) Filters			
F098M	Blue grism reference	982.93	169.48	0.97
F127M	H_2O/CH_4 continuum	1273.64	68.79	0.98
F139M	H_2O/CH_4 line	1383.80	64.58	0.98
F153M	H_2O and NH_3	1533.31	68.78	0.98
	IR Narrow-Band (N) Filters			
F126N	[Fe II]	1258.26	11.83	0.90
F128N	Paschen beta	1283.30	13.54	0.94
F130N	Paschen beta continuum	1300.62	13.28	0.96
F132N	Paschen beta (redshifted)	1319.04	13.07	0.91
F164N	[Fe II]	1645.13	17.48	0.93
F167N	[Fe II] continuum	1667.26	17.16	0.93
	IR Grisms (G)			
G102	"Blue" high-resolution grism	(1025)	250	
G141	"Red" low-resolution grism	(1410)	600	

1. See footnote 1 of Table 4 for naming conventions.
2. "Pivot wavelength" is defined as in Table 4.
3. Full width at 50% of peak transmission.

5.3 Anticipated WFC3 Performance

Table 6 presents the predicted limiting-magnitude performance of WFC3 and compares it with that of the ACS and NIC3 cameras. The calculations are based on a 3×3 pixel extraction box on a point source. The limiting ABMAG at a S/N of 10 was calculated for a 1-hour and a 10-hour exposure. The throughput curves for the WFC3 filters listed in column 2 were used; for ACS and NIC3, the most similar wide-band filter was used, and its name is given in column 3. The ACS/HRC camera was assumed for the NUV and *U*-band comparison; ACS/WFC was assumed for *B*, *V*, and *I*; and NIC3 for *J* and *H*. The FPA 129 IR detector was assumed for the WFC3/IR calculations.

An online exposure-time calculator (ETC) is planned for release in mid-2007 and will be linked on the WFC3 web site.

Table 6: Anticipated limiting-magnitude performance of WFC3 compared with those of ACS and NIC3. The table gives limiting ABMAGs at a S/N of 10 for the indicated WFC3 filters and for ACS or NIC3 for their most similar filters. WFC3 UVIS comparisons are with the ACS HRC channel (NUV and *U*) and the ACS WFC channel (*B, V, I*). WFC3 IR comparisons are with NIC3 (*J* and *H*).

Band	WFC3 Filter	ACS or NIC3 Filter	WFC3 limiting mag in 1 hr.	ACS or NIC3 limiting mag in 1 hr.	WFC3 limiting mag in 10 hr.	ACS or NIC3 limiting mag in 10 hr.
NUV	F225W	F220W	26.2	25.0	27.7	26.4
U	F300X	F330W	27.0	26.0	28.5	27.4
B	F438W	F435W	26.9	27.4	28.3	28.7
V	F606W	F606W	27.5	27.7	28.9	29.0
I	F814W	F814W	26.6	27.1	28.0	28.4
J	F110W	F110W	27.4	26.6	28.7	27.9
H	F160W	F160W	26.7	26.3	28.0	27.6

5.4 Parallel Observations

The ability of the *HST* system to support simultaneous operations with WFC3 and ACS, as well as possible enhancements of its data-volume capabilities, are still being evaluated as of this writing. Whether it will be possible to support parallel observations with WFC3 and ACS, therefore, is not known at this time.